Supporting Information

# Synthesis and Characterization of CIT-13, a Germanosilicate Molecular Sieve with Extra-large Pore Openings

Jong Hun Kang,[§] Dan Xie,[†] Stacey I. Zones,[†] Stef Smeets,[‡] Lynne B. McCusker[‡#], Mark E. Davis,[§]*

[§]Chemical Engineering, California Institute of Technology, Pasadena, CA 91125

[†]Chevron Energy Technology Co., 100 Chevron Way, Richmond, CA 94802

[‡]Department of Materials and Environmental Chemistry, University of Stockholm, Svante Arrhenius väg 16C, SE-106 91 Stockholm, Sweden

[#]Department of Materials, ETH Zurich, CH-8093, Zurich, Switzerland

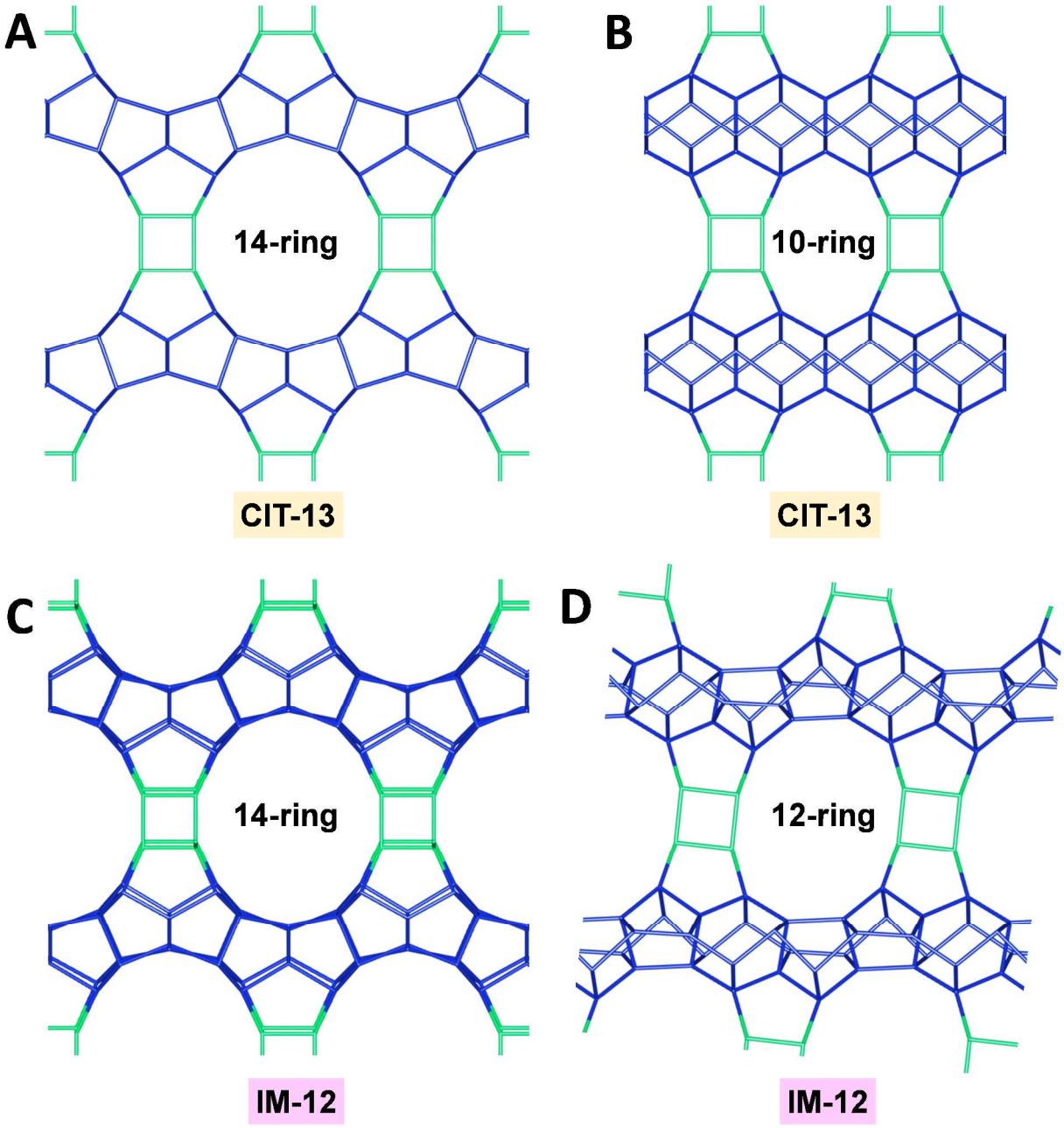


**Figure S1**. Comparison between the crystal structures of CIT-13 and IM-12. (A) CIT-13 viewed along the [001] direction showing the 14-ring pore, and (B) along the [010 direction showing the 10-ring pore. (C) IM-12 viewed along the [001] direction showing the 14-ring pore, and (D) along the [010] direction showing the 12-ring pore.

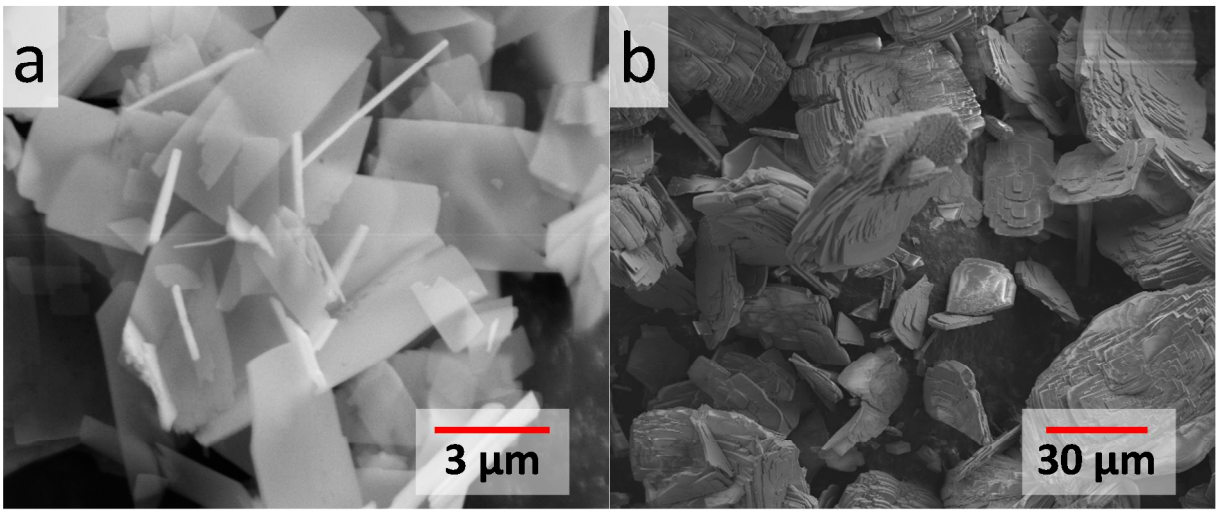


**Figure S2.** SEM micrographs of CIT-13 crystals prepared by heating (A) in a rotating autoclave and (B) in a static autoclave.

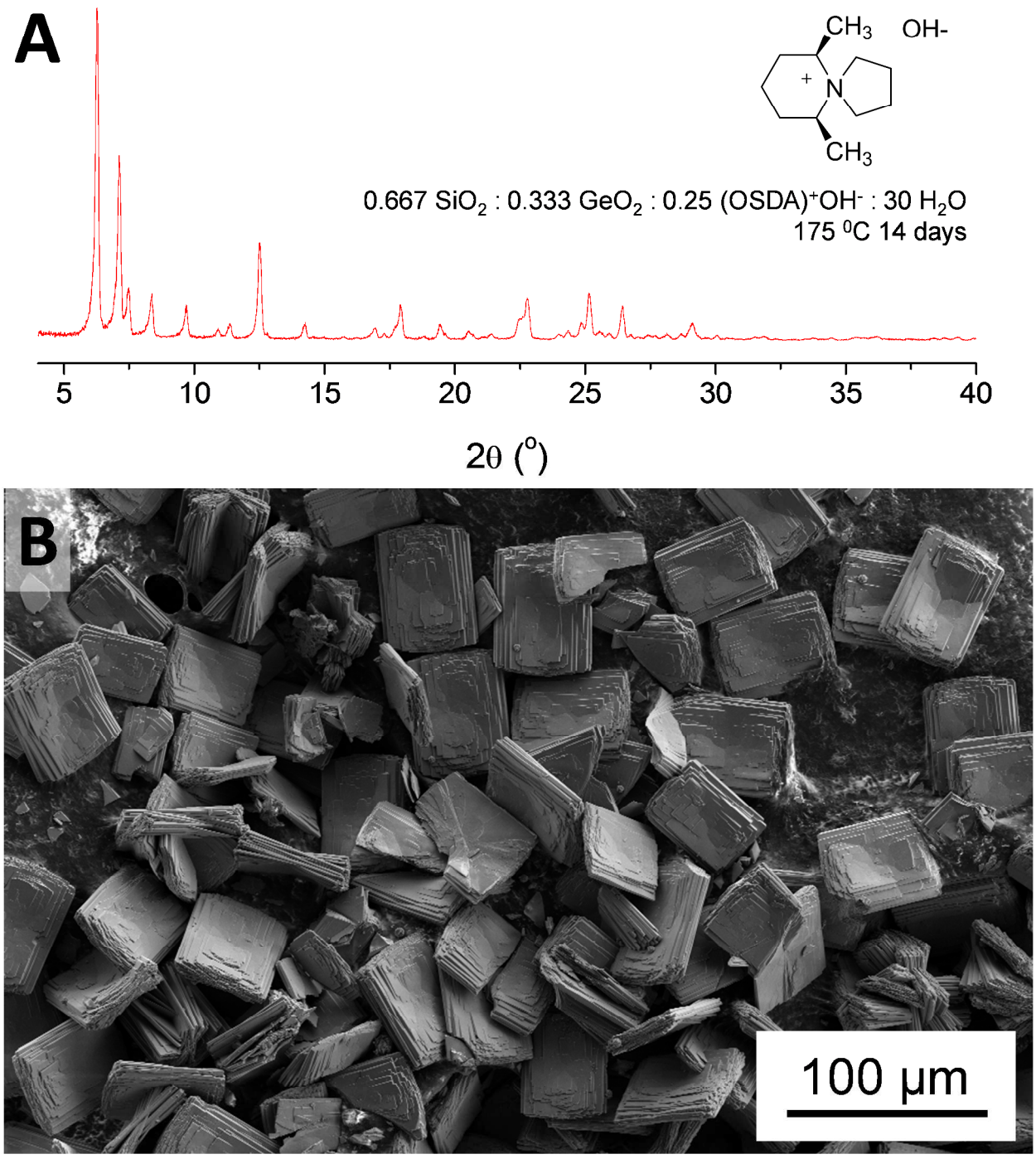


**Figure S3**. (A) An XPD pattern and (B) SEM image of a sample of the germanosilicate IM-12 synthesized in hydroxide medium (**UTL** framework type). The Si/Ge ratio was determined using EDS to be 4.5. This sample was used for comparison with CIT-13.

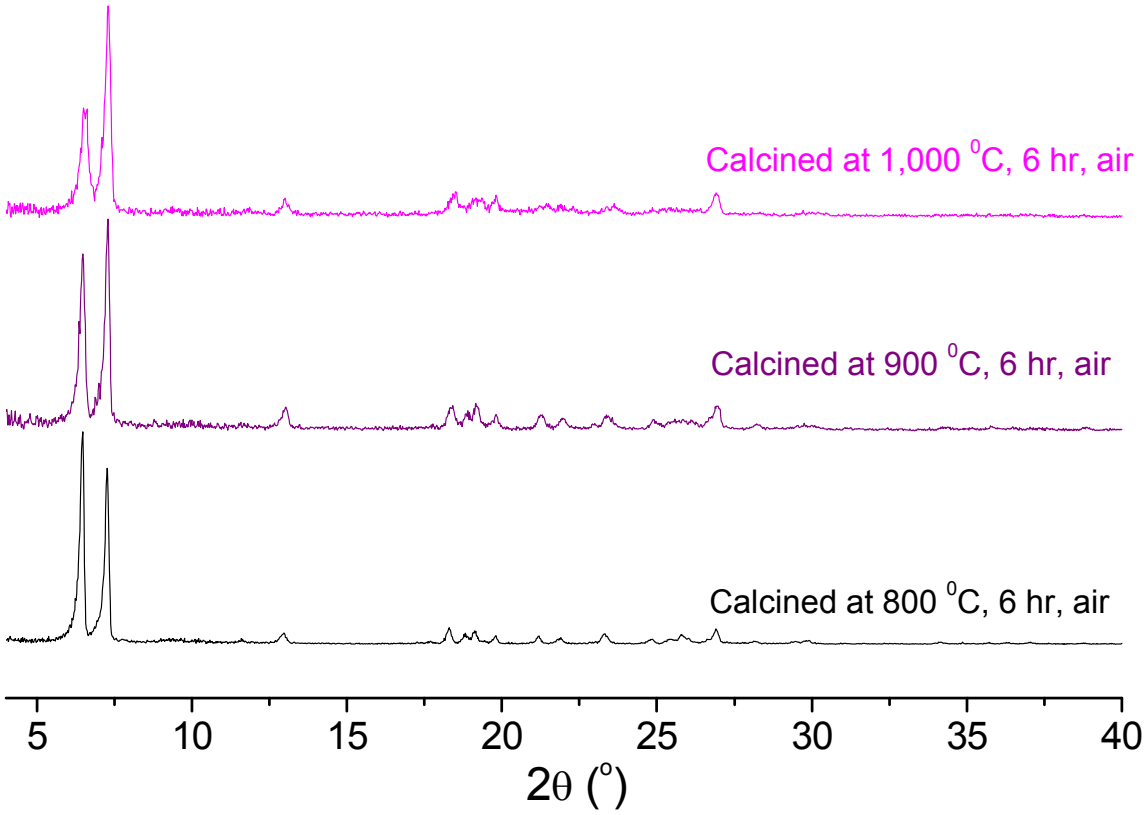


**Figure S4.** The XPD patterns of CIT-13 calcined in an air flow at high temperatures (800 °C to 1,000 °C) for 6 hours.

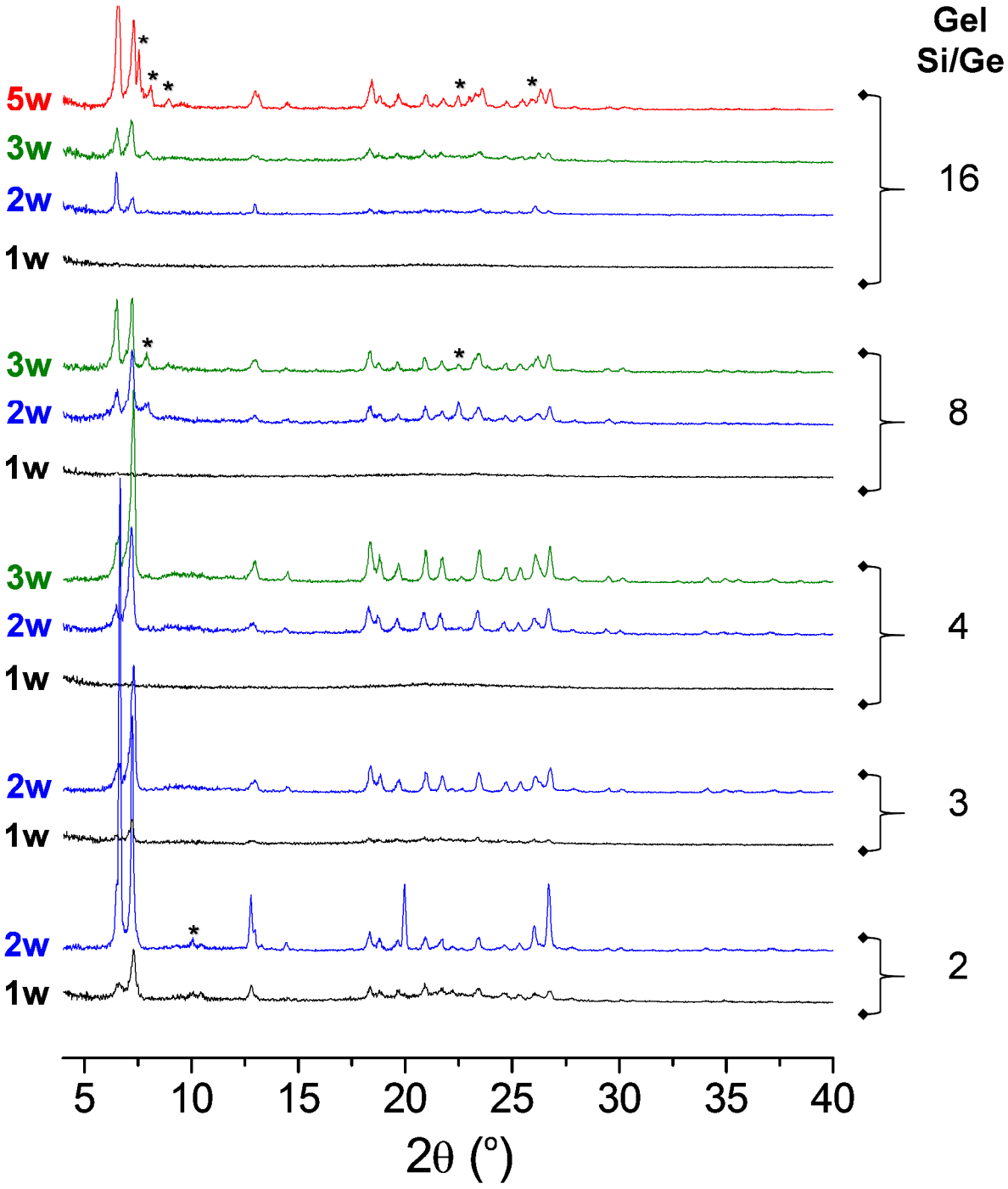


**Figure S5**. The effect of the Si/Ge ratio in the gel on the crystallization of CIT-13 (*: impurity; w: week).

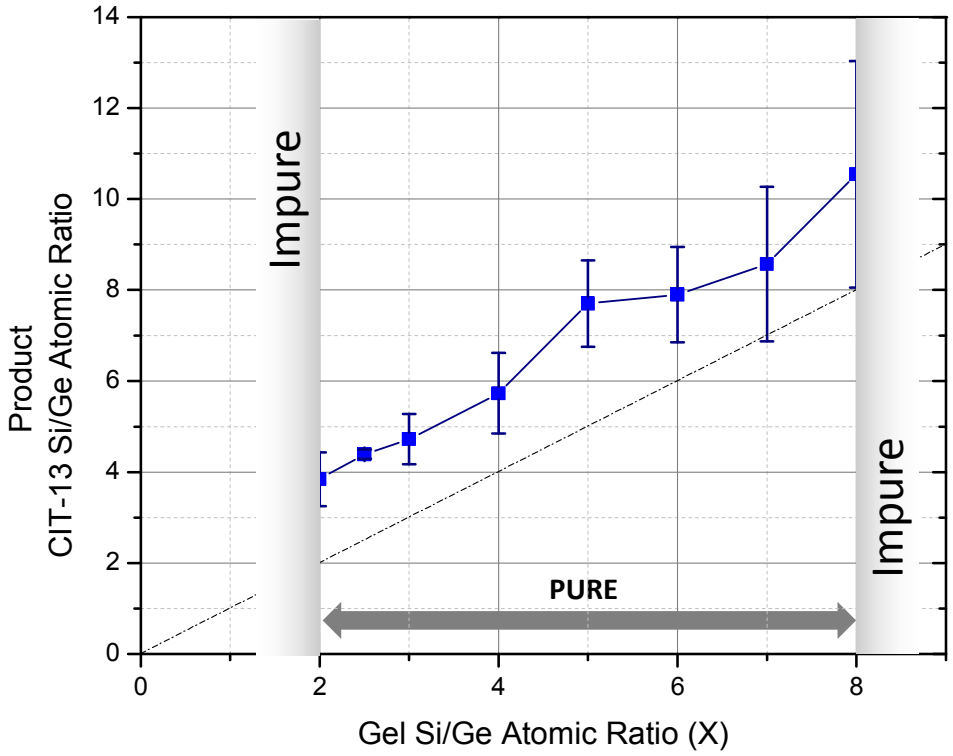


**Figure S6**. The relation between the gel Si/Ge ratios and the product CIT-13 Si/Ge ratios, characterized using the EDS.

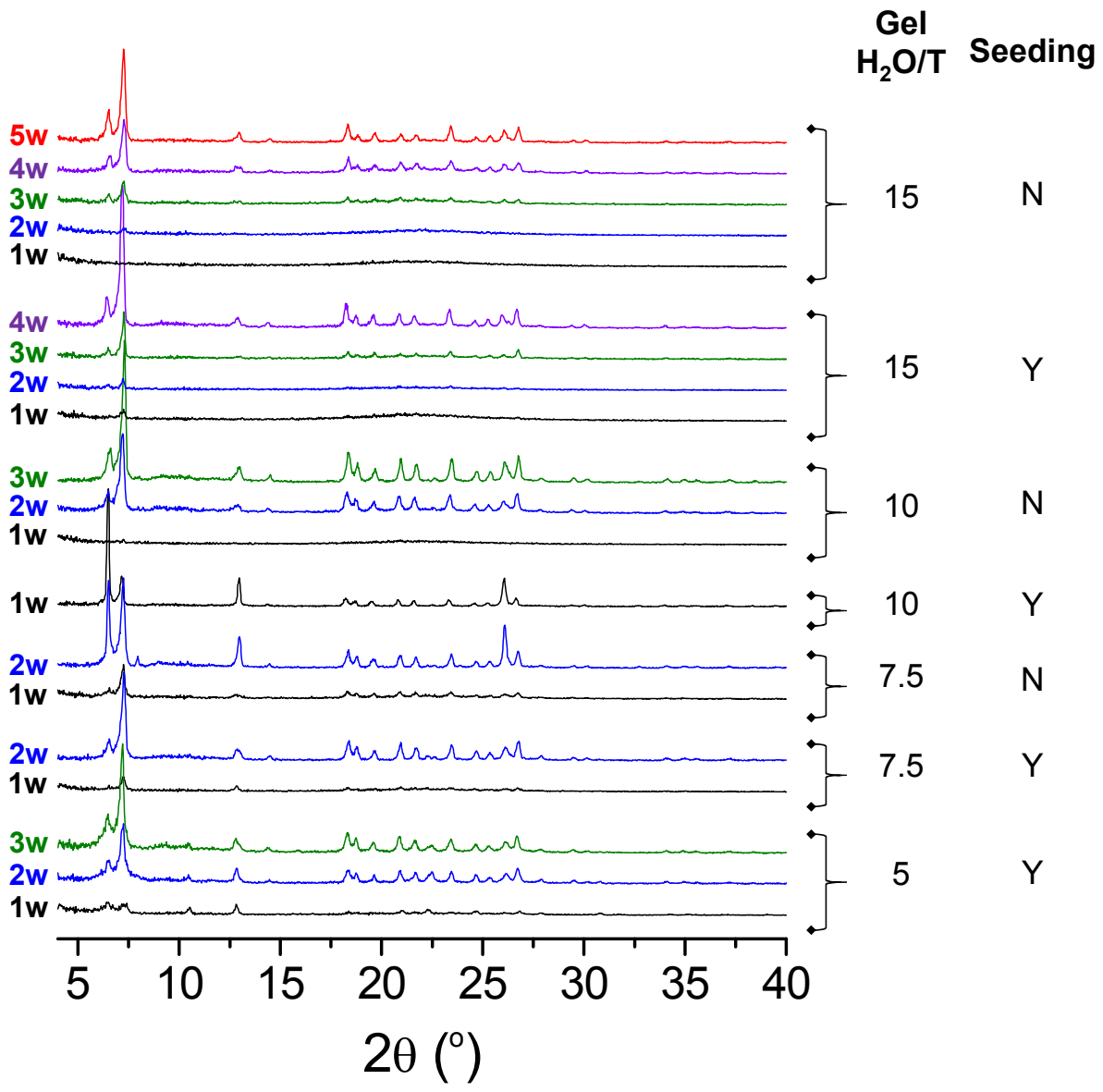


**Figure S7**. The effect of water levels in the gel on the crystallization of CIT-13 (w: week).

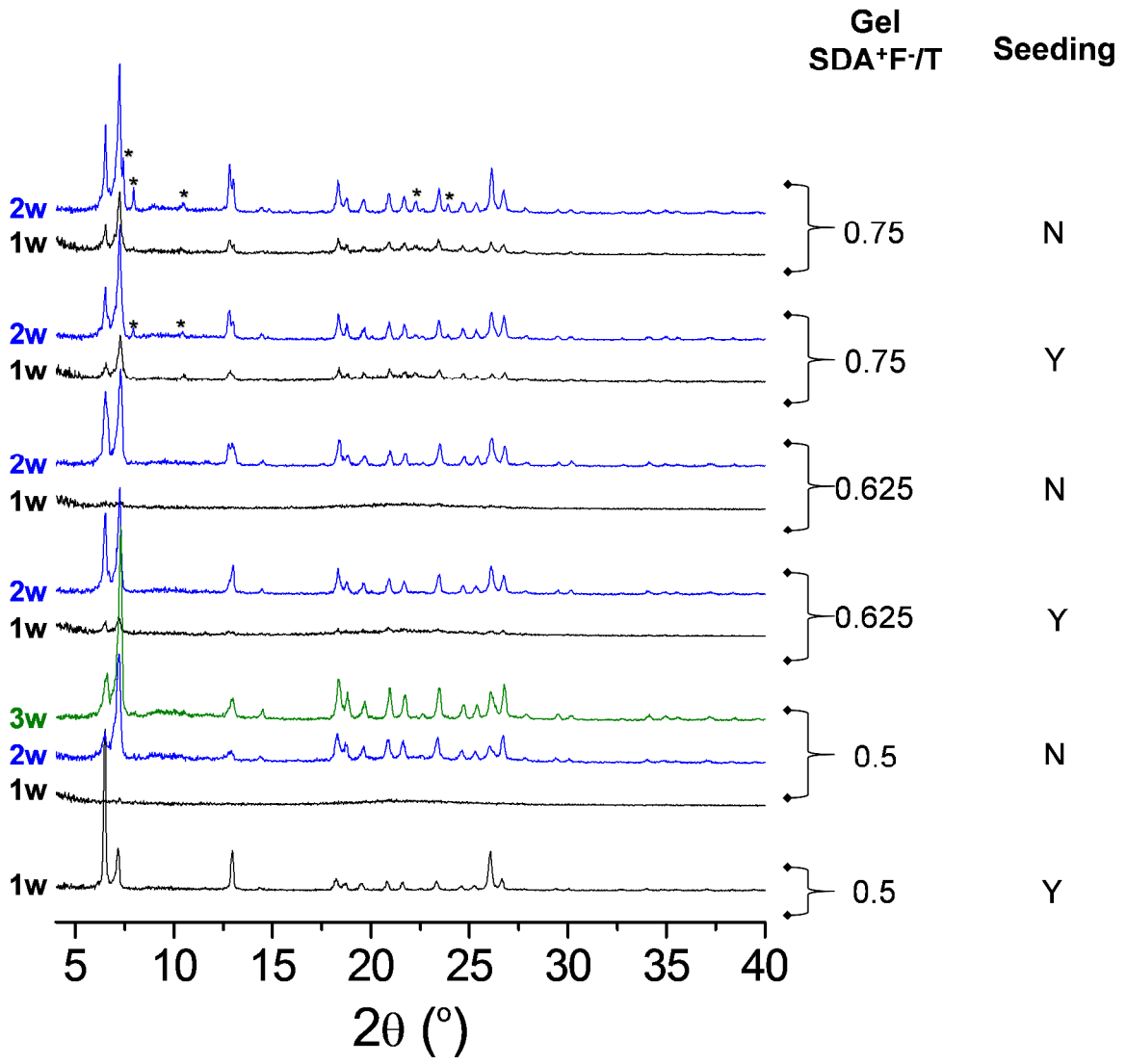


**Figure S8**. The effect of amount of OSDA in the gel on the crystallization of CIT-13 (*: impurity; w: week).

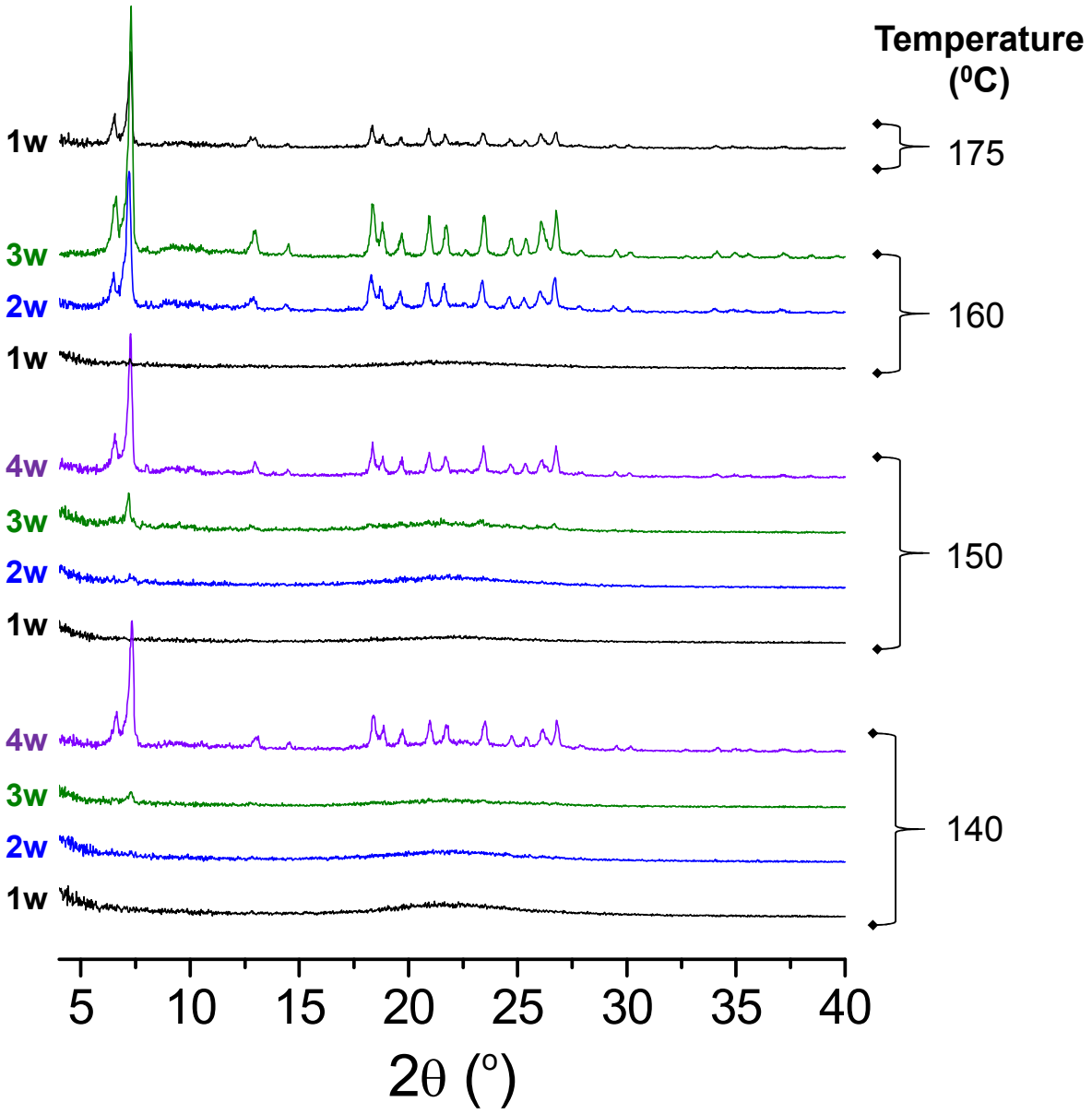


**Figure S9**. The effect of crystallization temperature on the crystallization of CIT-13 (*: impurity; w: week).

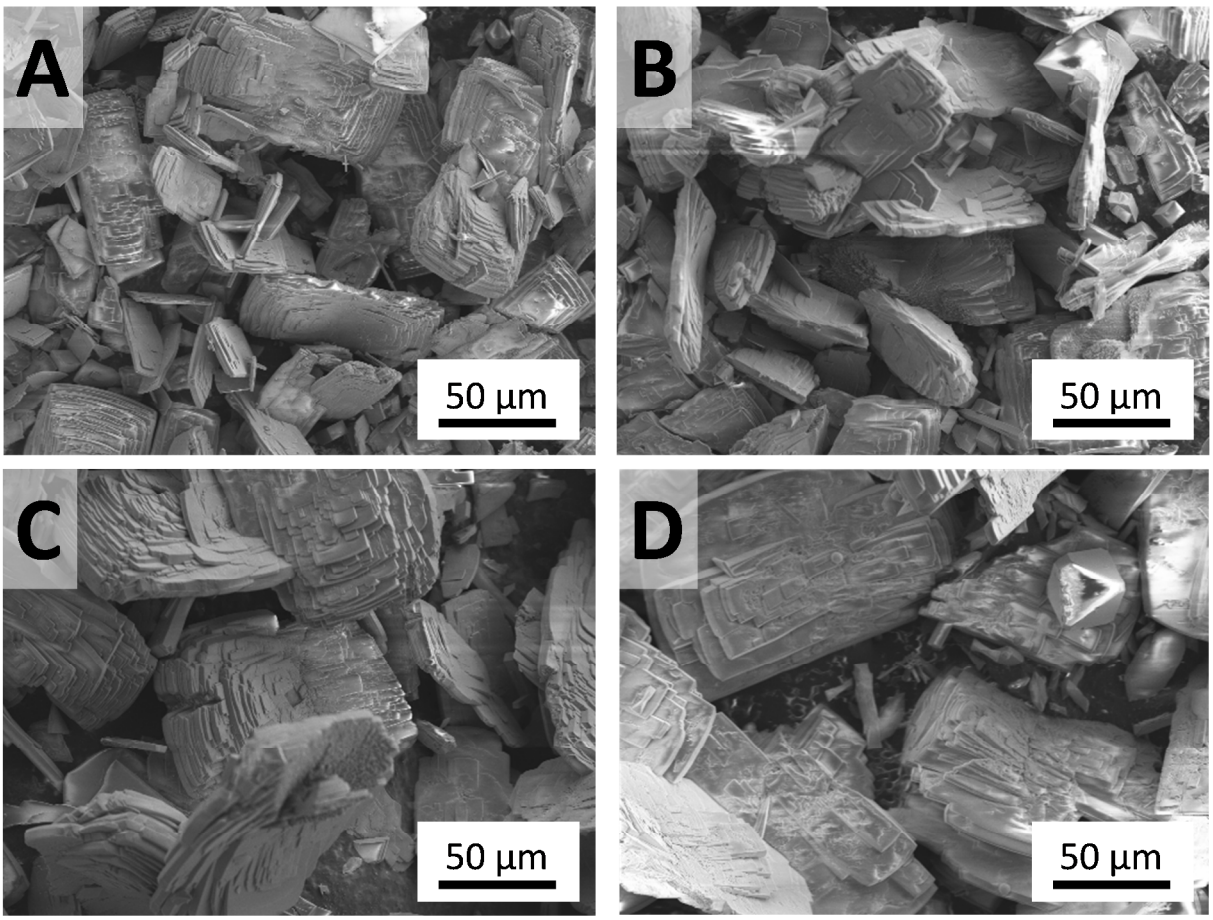


**Figure S10**. SEM micrographs of CIT-13 crystallized at (A) 140°C, (B) 150°C, (C) 160°C and (D) 175°C.

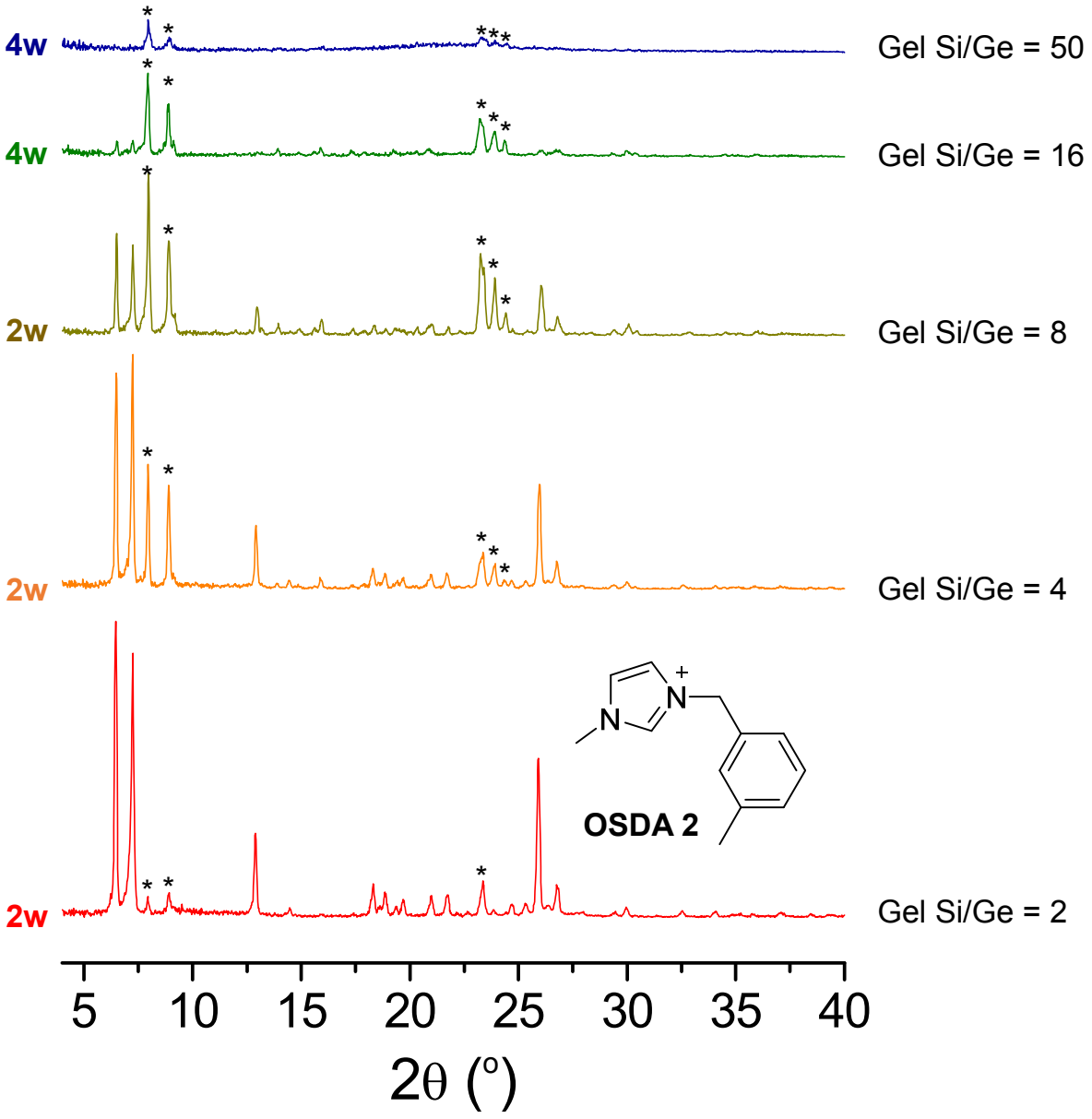


**Figure S11**. XPD patterns of germanosilicate samples that crystallized in the presence of **OSDA 2** and different Si/Ge ratios and in the gel (*: impurity; w: week). Here, the impurity phase was identified as an **MFI**-type material.

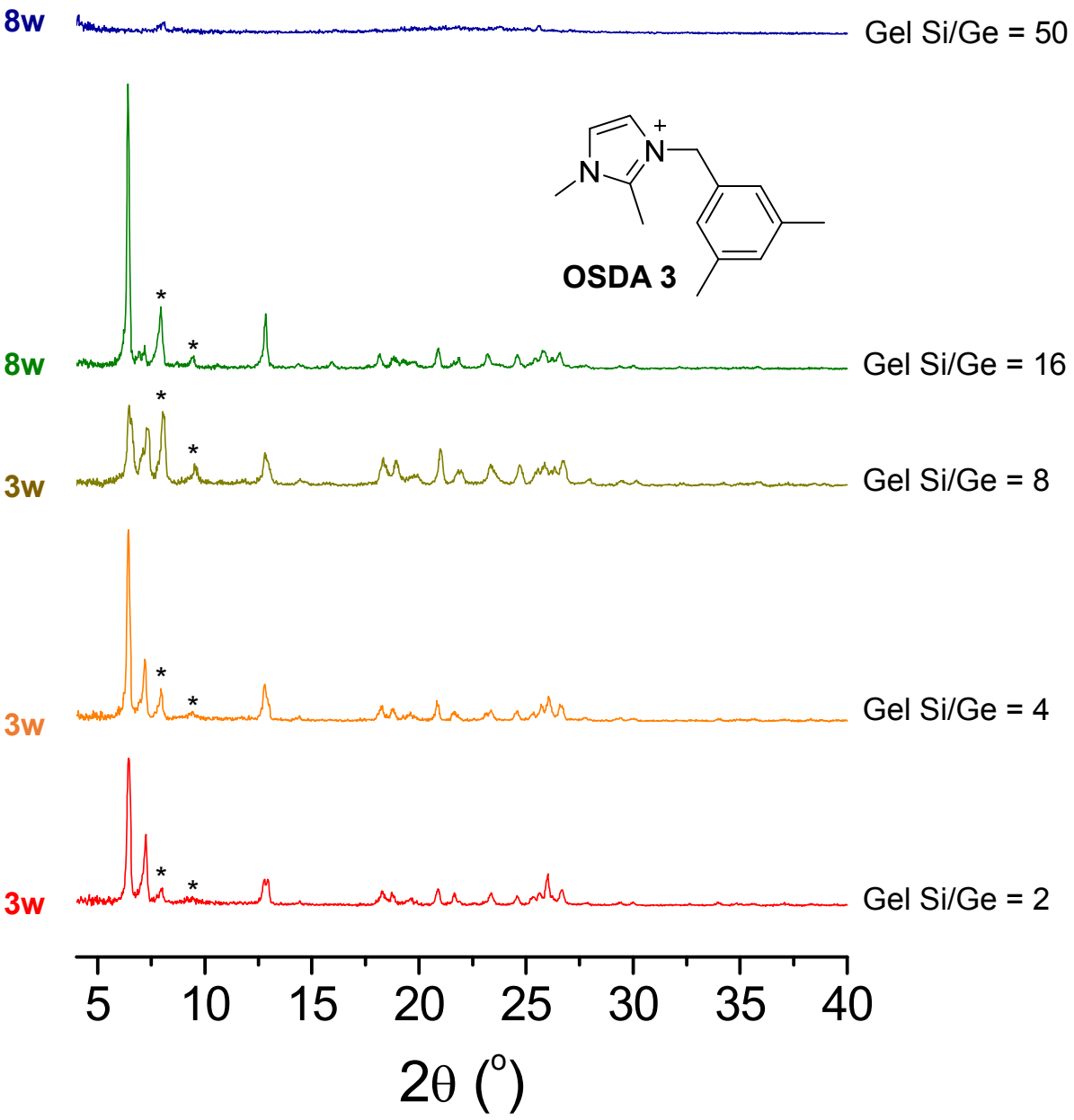


**Figure S12**. XPD patterns of germanosilicate samples that crystallized in the presence of **OSDA 3** and different Si/Ge ratios and in the gel (*: impurity; w: week).

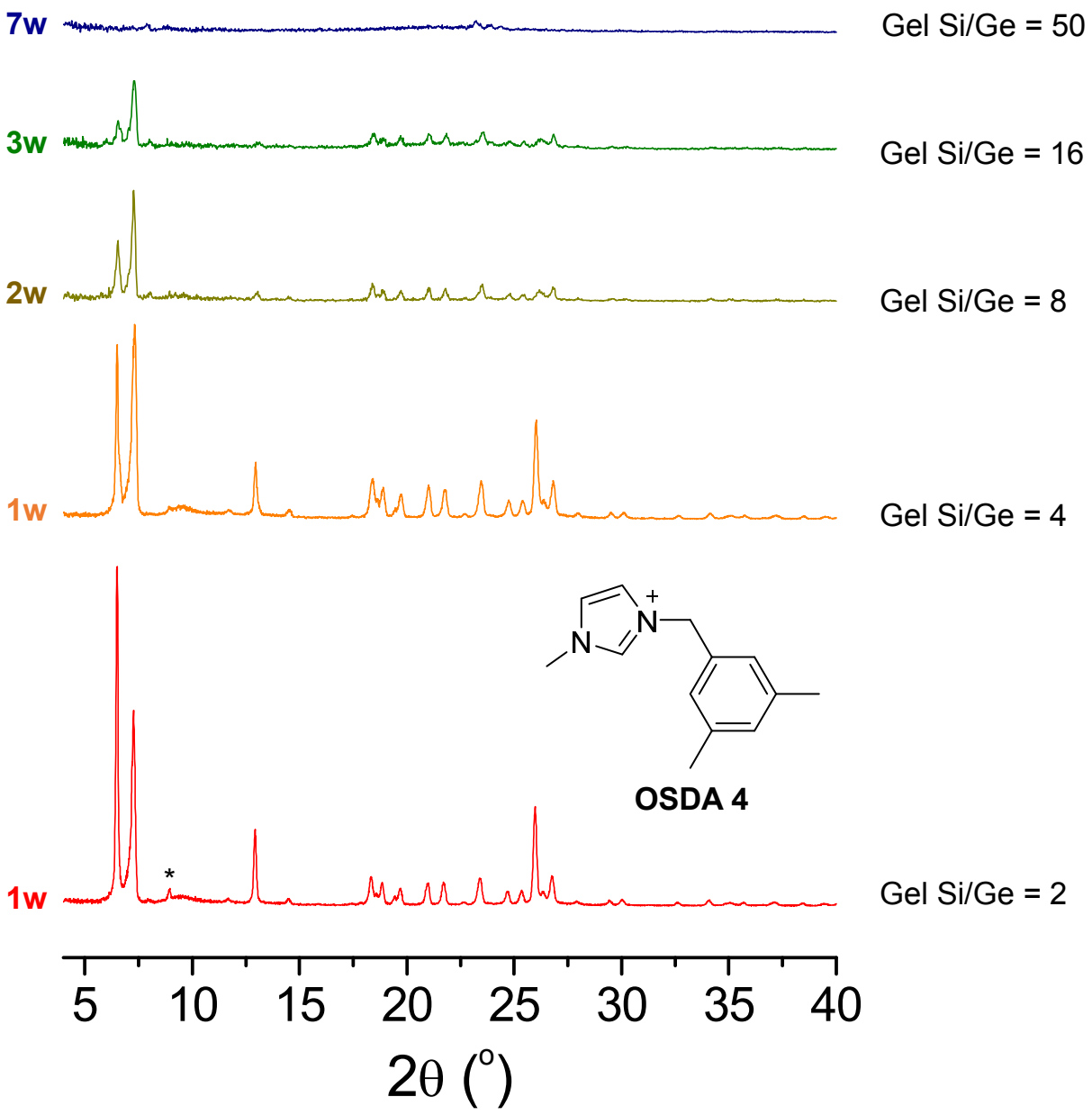


**Figure S13**. XPD patterns of germanosilicate samples that crystallized in the presence of **OSDA 4** and different Si/Ge ratios and in the gel (*: impurity; w: week).

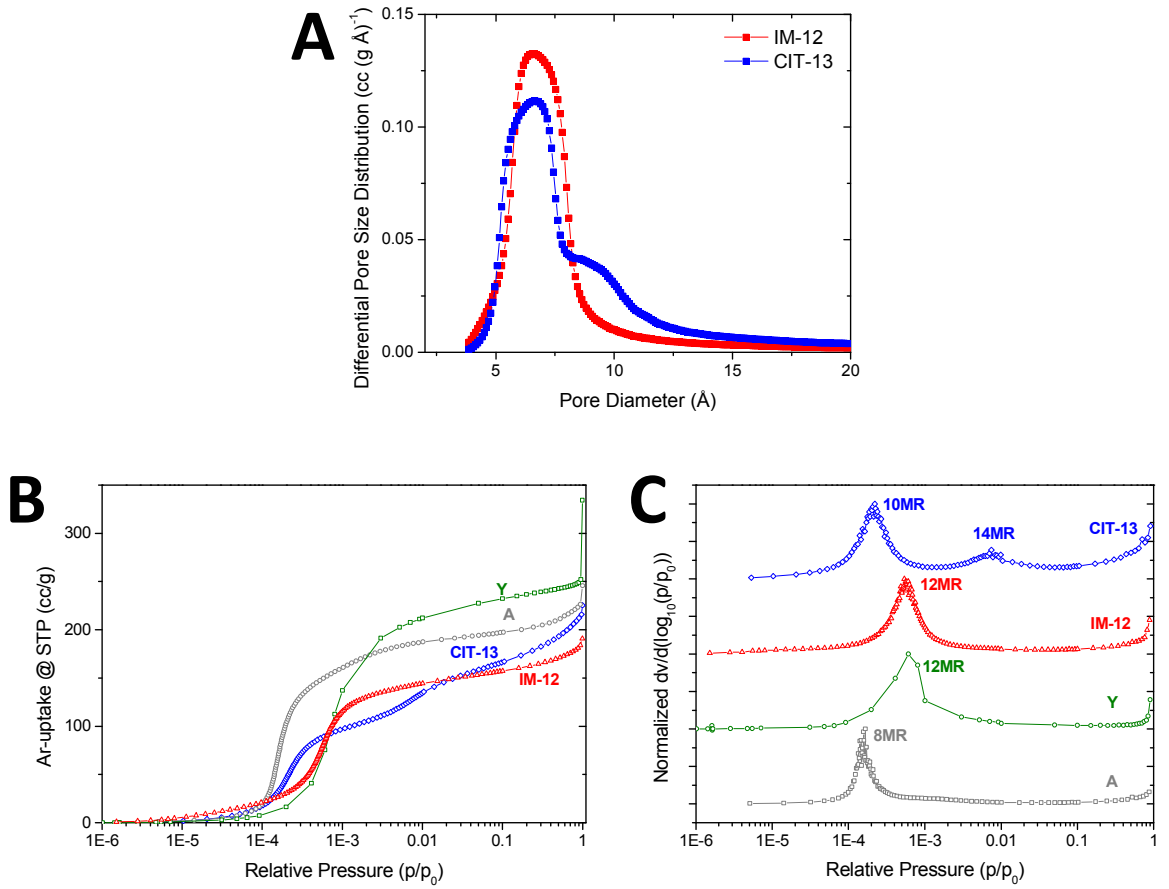


**Figure S14**. (A) The Saito-Foley pore size distribution derived from the argon adsorption isotherm shown in Figure 8. (B) The log-plot of the Ar-isotherms of CIT-13, IM-12, zeolite Y and zeolite A. (C) The normalized differentiated log-plot of isotherms in (B) to allow a qualitative comparison. *Zeolite Y and Zeolite A data courtesy of Dr. Joel E. Schmidt.*

Since the small micropores are filled with argon atoms at a lower pressure then the large micropores, the position at which the inflection point in the log-plot is observed allows the pore size to be estimated qualitatively. For zeolite A (**LTA**) and zeolite Y (**FAU**), the inflection points are observed at $p/p_0 = 10^{-3.80}$ and $10^{-3.22}$ (Figure S13B and C), and these correspond to 8-rings and 12-rings, respectively. IM-12 (**UTL**) shows the inflection point at $p/p_0 = 10^{-3.26}$, which is very close to that of zeolite Y, so this inflection point was assigned to 12-rings in IM-12. CIT-13 was the only framework that showed two inflection points. The first was observed at $p/p_0 = 10^{-3.66}$ and assigned to the 10-rings and the second at $p/p_0 = 10^{-2.13}$ to the 14-rings. This second inflection point corresponding to 14-ring was not observable in IM-12.

**Table S1.** Crystallographic details for the structure refinement of as-synthesized CIT-13.

| **Sample** | **CIT-13** |
|---|---|
| **Chemical composition** | $\|(C_{13}N_2)_{3.30}F_2\|[Si_{54.34}Ge_{9.66}O_{128}]$ |
| **Space group** | *Cmmm* |
| ***a* (Å)** | 27.4374(5) |
| ***b* (Å)** | 13.8000(2) |
| ***c* (Å)** | 10.2910(2) |
| ***V* (Å$^3$)** | 3896.6(1) |
| ***Z*** | 8 |
| **$\rho$ (g/cm$^3$)** | 2.144(2) |
| **$\lambda$ (Å)** | 0. 776381(1) |
| **2$\theta$ range (°)** | 2.0–46.0 |
| $R_I$ | 0.0126 |
| $R_{wp}$ | 0.0773 |
| $R_{exp}$ | 0.0015 |
| **Observations** | 16899 |
| **Reflections** | 1241 |
| **Parameters** | 104 |
| **Geometric restraints** | 62 (zeolite)<br>38 (SDA) |

**Table S2.** Selected bond lengths and angles (Å, °).

| | | **T–O–T** | **O–T–O** | **T–O** |
|---|---|---|---|---|
| **CIT-13** | min | 138.3 | 107.8 | 1.55 |
| | max | 180.0 | 113.8 | 1.63 |
| | avg | 156.6 | 109.6 | 1.59 |

Restraints used: T–O–T: 135±10°; O–T–O: 109.5±0.8°; T–O: 1.61±0.01 Å; $w=1/\sigma^2$